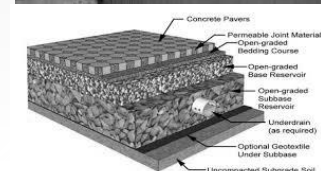
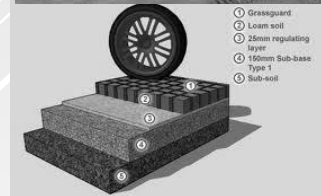
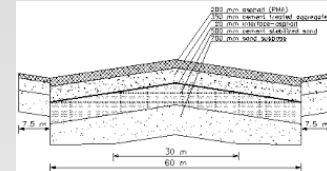


LECTURE 6:

Axle loads, wheel loads and contact pressures



6.1 Axle loads

In order to be able to design a pavement structure, knowledge on the magnitude of the traffic loads is essential. Axle load measurements are therefore made to determine the number and weight of the axles passing over the pavement. Axle load measurements can be made in different ways varying between the up to date system shown in figure 50, to the much more simple system shown in figure 51.

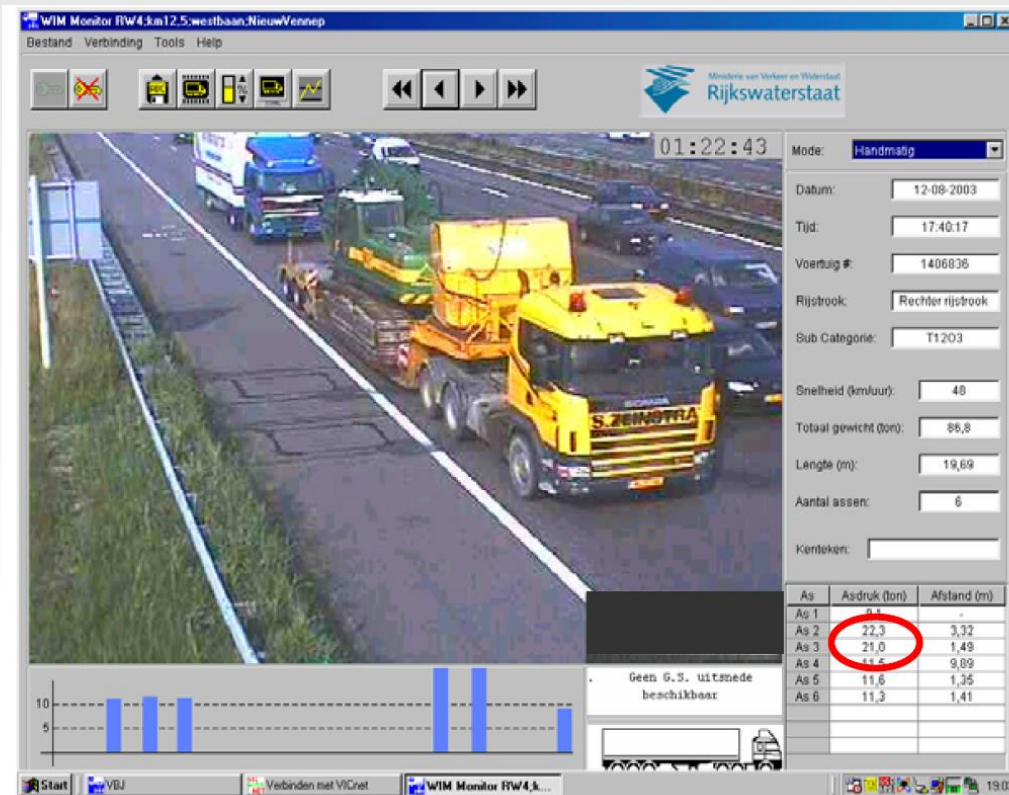


Figure 50: Example of a modern axle load survey unit as used in the Netherlands.



Figure 51: Simple axle load unit as used for surveys in Ghana

- The system as shown in figure 50 uses piezoelectric and coax cables to measure the axle load and other features of the truck. Such features include the speed of the truck as well as its registration number. Other items are the distance between the axles, the total length of the vehicle and a classification is made of the type of truck.
- This example shows amongst other things that the heaviest axle load is the tandem axle of the truck. The second axle from the front end of the truck was carrying a load of 223 kN (22.3 tons) while the third axle from the front carried 210 kN (21 tons). Comparing these values with the axle load regulations that prevail in the Netherlands (table 7), shows that the tandem axle is severely overloaded.

Maximum axle load driven axles (no restrictions with respect to suspension system, tires and steering)	115 kN
Maximum axle load non driven axles	100 kN
Maximum axle load tandem axles	
Axle distance < 1.0 m	100 kN
1.0 m ≤ axle distance < 1.3 m	160 kN
1.3 m ≤ axle distance < 1.8 m without air suspension system	180 kN
1.3 m ≤ axle distance < 1.8 m with air suspension system	190 kN
Maximum axle load triple axles	
Axle distance < 1.3 m	210 kN
1.3 m ≤ axle distance < 1.8 m without air suspension system	240 kN
1.3 m ≤ axle distance < 1.8 m with air suspension system	270 kN

Table 7: Axle load regulations in the Netherlands.

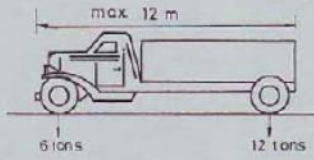
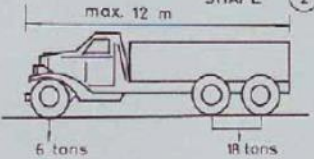
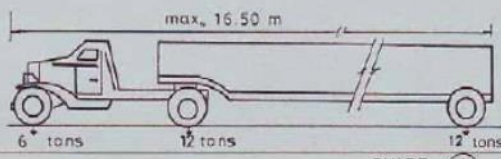
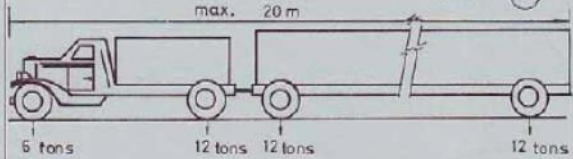
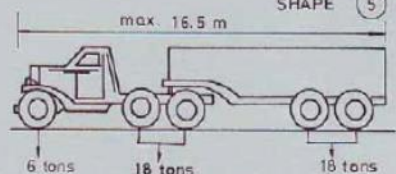
Legal Limits of Commercial Vehicle Weights and Sizes for Iraq

[illegible]

3 THE VEHICLE

FIGURE I-18a

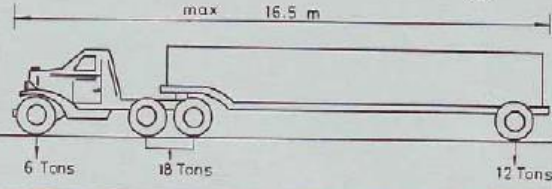
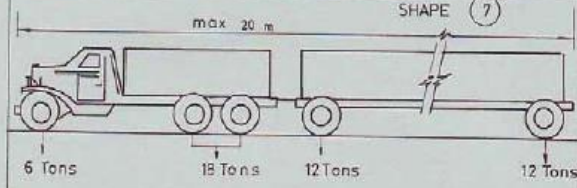
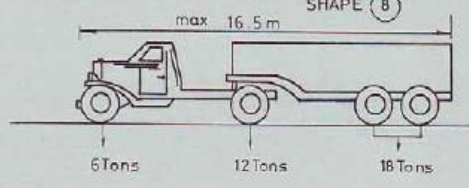
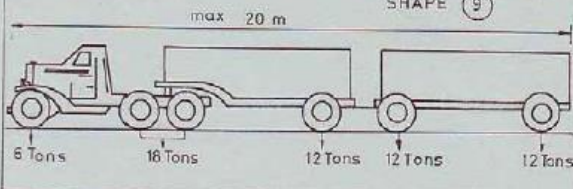
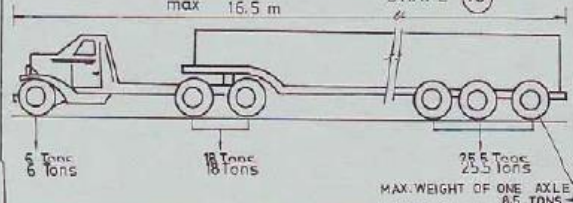
Legal Axle and Gross Weights Permitted on Motor Vehicles in Regular Operation in Iraq

MAXIMUM GROSS WEIGHT	VEHICLE TYPE	SHAPE ①
18 tons	type 2	
24 tons	type 3	
30 tons	type 2-S1	
42 tons	type 2-2	
42 tons	type 3-S2	

3 THE VEHICLE

FIGURE I-18b

Legal Axle and Gross Weights Permitted on Motor Vehicles in Regular Operation in Iraq

MAXIMUM GROSS WEIGHT	VEHICLE TYPE	SHAPE ⑥
36 tons	type 3-S1	
48 tons	type 3-2	
36 tons	type 2-S2	
60 tons	type 3-S1-2	
49.5 tons	type 3-S3	

- Figure 51 shows the axle load unit that was used in Ghana during an axle load survey program sponsored by the European Union [17]. The unit consisted of 4 Haenni WL 103 scales which were arranged in such a way that first the outer wheel of an axle were weighed and after that the total axle weight. This measurement procedure allowed to determine whether or not all the wheels of an axle were carrying the same load.

Table 8 shows the axle load distributions as they are used in the Netherlands as input for the thickness design of concrete pavements [18]. Table 8 is also suggested for use for the design of flexible pavements.

Axle load group (kN)	Average wheel load P (kN)	Axle load frequency distribution (%) for different types of road						
		heavily loaded motorway	normally loaded motorway	heavily loaded provincial road	normally loaded provincial road	municipal main road	rural road	public transport bus lane
20-40	15	20.16	14.84	26.62	24.84	8.67	49.38	-
40-60	25	30.56	29.54	32.22	32.45	40.71	25.97	-
60-80	35	26.06	30.22	18.92	21.36	25.97	13.66	-
80-100	45	12.54	13.49	9.46	11.12	13.66	8.05	-
100-120	55	6.51	7.91	6.50	6.48	8.05	2.18	100
120-140	65	2.71	3.31	4.29	2.70	2.18	0.38	-
140-160	75	1.00	0.59	1.64	0.83	0.38	0.38	-
160-180	85	0.31	0.09	0.26	0.19	0.38	0.00	-
180-200	95	0.12	0.01	0.06	0.03	0.00	0.00	-
200-220	105	0.03	0.01	0.03	0.00	0.00	0.00	-
Av. nr. of axles per heavy vehicle		3.5	3.5	3.5	3.5	3.5	3.1	2.5

Table 8: Axle load distributions as used in the Netherlands for the design of concrete pavements.

Table 9 shows the results of the axle load survey in Ghana as reported in [17].

- The results were obtained by means of axle load surveys carried out in Ghana on different roads. In total 787 trucks were surveyed. The trucks had either 2, 3, 4, 5 or 6 axles. The axle loads, including the number 1 steering axle, are reported in table 9. The table also shows the maximum axle load measured, as well as the average axle load and the standard deviation. Given the fact that the allowable was 100 kN, it is quite clear that severe overloading occurred. This however, is a problem in many countries.
- The table also shows interesting information with respect to the tire pressures. Normally tires as surveyed should operate at an inflation pressure of around 700 kPa. The table shows that the mean tire pressure was indeed close to this value but also that some very exotic values occurred. These high tire pressures certainly result in high contact stresses and in accelerated pavement damage.

Axle load	Axle 1	Axle 2	Axle 3	Axle 4	Axle 5	Axle 6
10	1	0	0	0	0	0
20	5	0	0	0	0	0
30	42	3	3	1	0	0
40	110	8	8	7	3	0
50	144	11	13	12	4	0
60	222	33	39	23	4	0
70	123	56	40	27	4	0
80	80	77	63	44	5	0
90	35	68	78	32	4	0
100	21	81	70	48	3	0
110	4	81	49	30	4	0
120	0	86	59	28	9	1
130	0	57	24	19	0	0
140	0	46	39	25	7	0
150	0	41	14	19	4	1
160	0	39	6	4	1	0
170	0	41	5	2	1	0
180	0	28	2	2	2	0
190	0	13	1	5	2	0
200	0	9	0	0	2	0
210	0	5	0	0	0	0
220	0	2	0	0	0	0
230	0	2	0	0	0	0
240	0	1	0	0	0	0
axle load summary [kN]						
max	112,5	236,5	189,0	191,5	203,5	153,5
avg	59,97	116,08	99,08	101,25	108,96	135,5
sa	16,77	38,06	28,43	31,75	43,10	25,46
tire pressure [kPa]						
max	1050	1015	980	980	945	840
avg	756	798	805	819	826	840
sa	105	77	63	56	49	0

Table 9: Results of axle load surveys in Ghana.

Table 10 shows results of axle load measurements as performed in Yemen. Again one notices the large amount of very heavy, overloaded, vehicles.

Vehicle type	Axle	Axle load range [kN]		
		Min.	Max.	Average
Heavy busses (1%) vehicle weight	1	30	58	46
	2	49	107	84
		82	164	130
2 axle medium truck (34%) vehicle weight	1	33	63	47
	2	75	144	115
		115	191	162
2 axle heavy truck (30%) vehicle weight	1	33	99	70
	2	98	243	170
		145	343	240
3 axle truck (30%) vehicle weight	1	42	109	74
	2	67	226	153
	3	76	240	161
		187	553	388
4 axle truck (3%) vehicle weight	1	45	79	60
	2	80	202	134
	3	80	180	133
	4	92	193	136
		227	595	395
5 axle truck (2%) vehicle weight	1	44	89	67
	2	52	161	110
	3	52	169	109
	4	68	204	142
	5	70	201	151
		327	736	577

Table 10: Axle loads for the Hodeidah – Sanaa road [19].

Note: the percentages given are the percentages of occurring.

Table 11 is another example of overloading conditions. The results presented in that table are from axle load surveys done on the Jing-Zhu freeway in the Hubei province, China [20]. The table not only shows a significant amount of overloading (legal load limit is 100 kN) but also clearly indicates that the overload problem rapidly increased during the 1995 – 1998 period.

Year	Axle load (kN)													
	< 60		60-100		100-130		130-150		150-180		>180		total	
	no.	%	no.	%	no.	%	no.	%	no.	%	no.	%	no.	%
1995	893	25.86	811	23.49	811	23.49	420	12.16	352	10.19	166	4.81	3453	100
1996	899	20.26	1027	23.15	1026	23.14	665	14.99	557	12.55	263	5.93	4437	100
1997	981	18.74	1218	23.26	1217	23.24	815	15.57	682	13.02	322	6.15	5235	100
1998	1078	17.66	1193	19.54	1192	19.52	1183	19.38	991	16.23	468	7.67	6105	100

Table 10: Axle loads on the Jing-Zhu freeway in China.

- From the information given so far, it is clear that an as good as possible estimation of the axle load distribution is essential. Overloading seems to be a problem in many countries and one should realize that especially the heavy, overloaded vehicles are causing most of the pavement damage.
- At this moment it is appropriate to recall the concept of load equivalency. This concept implies that one determines the damaging effect of a particular axle load relative to a standard axle load. The equivalent number of load repetitions is calculated using:

$$N_{eq} = (L/L_{ref})^m N_L$$

Where:

N_{eq} = number of equivalent passages of the axle load considered,

L = axle load to be considered,

L_{ref} = reference axle load,

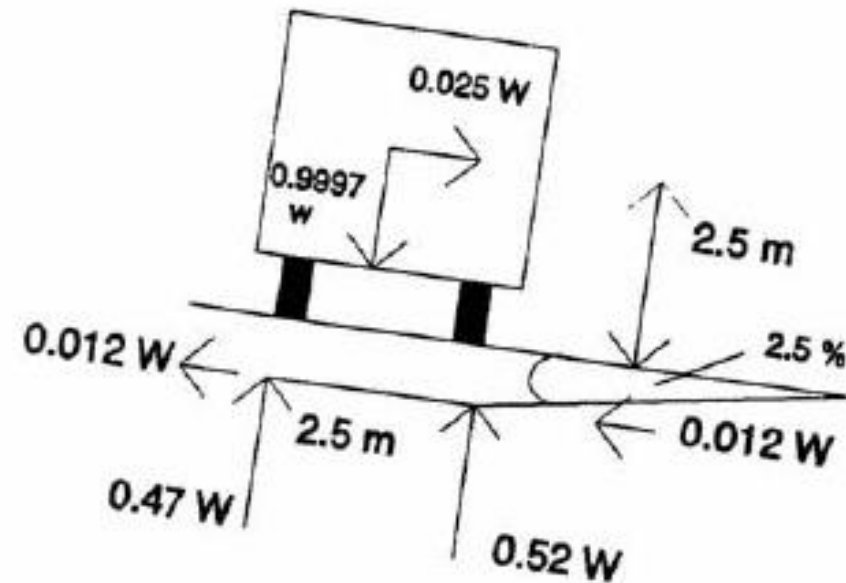
N_L = number of repetitions of the axle passages considered,

m = damage factor.

- The equation implies that if the reference axle equals 100 kN and assuming $m = 4$, a 200 kN axle produces 16 times more damage than the reference axle does. It should be noted that the value of m depends on which damage type is considered. If one wants to know the damaging effect of various axle loads relative to each other in terms of fatigue of the asphalt layer, then $3 < m < 6$. If the effect on fatigue in a cement treated layer has to be considered, then $7 < m < 10$. If the effect on the loss of serviceability needs to be considered then $m = 4$.

6.2 Wheel loads

One would expect that the wheel load is equal to the axle load divided by the number of wheels on the axle. This however is not true. Figure 52 e.g. shows that chamber of the pavement surface results in an unequal sharing of the axle load over both wheel groups of the axle.



W = Weight of the vehicle

Figure 52: Chamber of the roads results in unequal sharing.

The wheel group on the verge side of the road carries 52% of the load while the wheel group near the centre line of the road carries 47%. Wheel load measurements as carried out in Ghana [17] showed however that quite often the axle load was far from equally distributed over the wheels of the axle; some examples are shown in figure 53.

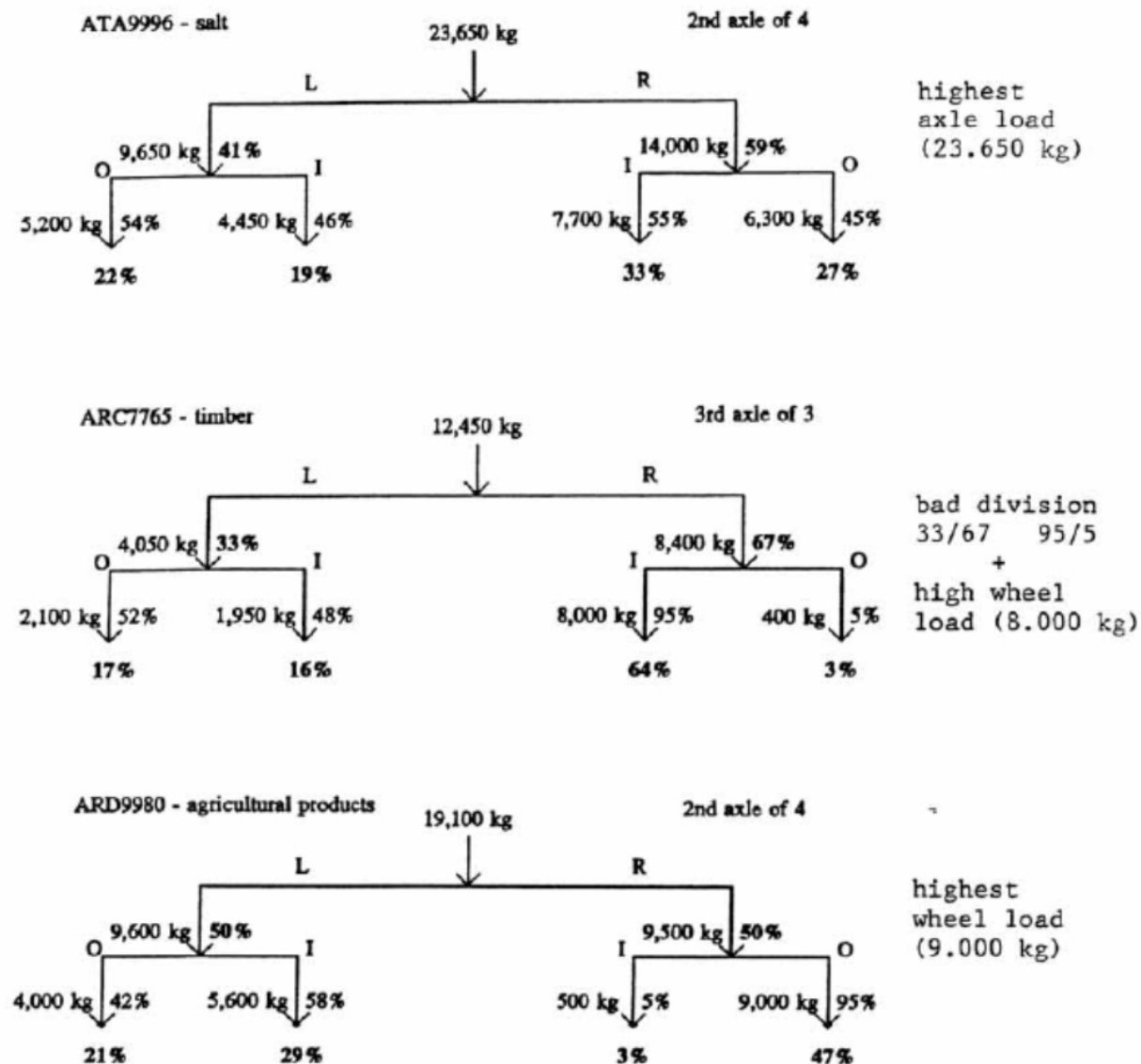


Figure 53: Examples of unequal sharing of the axle load over the wheels.

6.3 Contact pressures

- As mentioned before, knowledge on axle and wheel loads is important but even more so is knowledge on the contact pressures. Wheel loads come in different sizes and shapes, some of them are shown in figure 54, and each of them produces a different contact pressure distribution.
- The well known dual tire configuration is shown on the left of figure 54; it is used all over the world for the driven and towed axles. Normally these tires have an inflation pressure of around 700 kPa. The steering axle of a truck always has a single tire, having the same dimensions as one of the dual tires.
- In western Europe however, most of the towed axles are equipped nowadays with a so called wide base or super single tire. This tire is shown on the far right of the picture. Normally the tire has an inflation pressure of 800 – 850 kPa.
- Next to the super single tire, the super super single tire is shown. This tire is still under development but will be used under the driven axle of trucks thereby replacing the dual wheel configuration. In between the super super single and the dual wheel is a small size dual wheel. This tire is not very much used yet. The idea behind it was that a smaller size tire would allow lowering the loading platform resulting in a larger loading capacity.



Figure 54: Different tire types.

In order to avoid excessive wear to the tire, the tire pressure should be selected in relation to the tire load. The following relationships can be used for this.

- The pressure used in the tires for dual wheels (1 axle has two dual wheels on either side of the axle; total nr. of wheels = 4) can be estimated from:

$$p = 0.35 + 0.0035 L$$

Where:

p = tire pressure [MPa],

L = axle load [kN].

- The pressure in the super single tires (1 axle has one wheel on either side of the axle; total nr. Of wheels = 2) can be estimated using:

$$p = 0.42 + 0.0038 L$$

The units in this equation are the same as used in the previous equation.

The consequences of less optimal combinations of tire load and tire pressure are shown in figure 55. This figure shows that when the tire pressure is too low, the tire walls are carrying most of the load. This can result in rather high contact pressures. The combination of a 50 kN load with a 520 kPa pressure results in contact pressures under the wall of the tire of approximately 900 kPa.

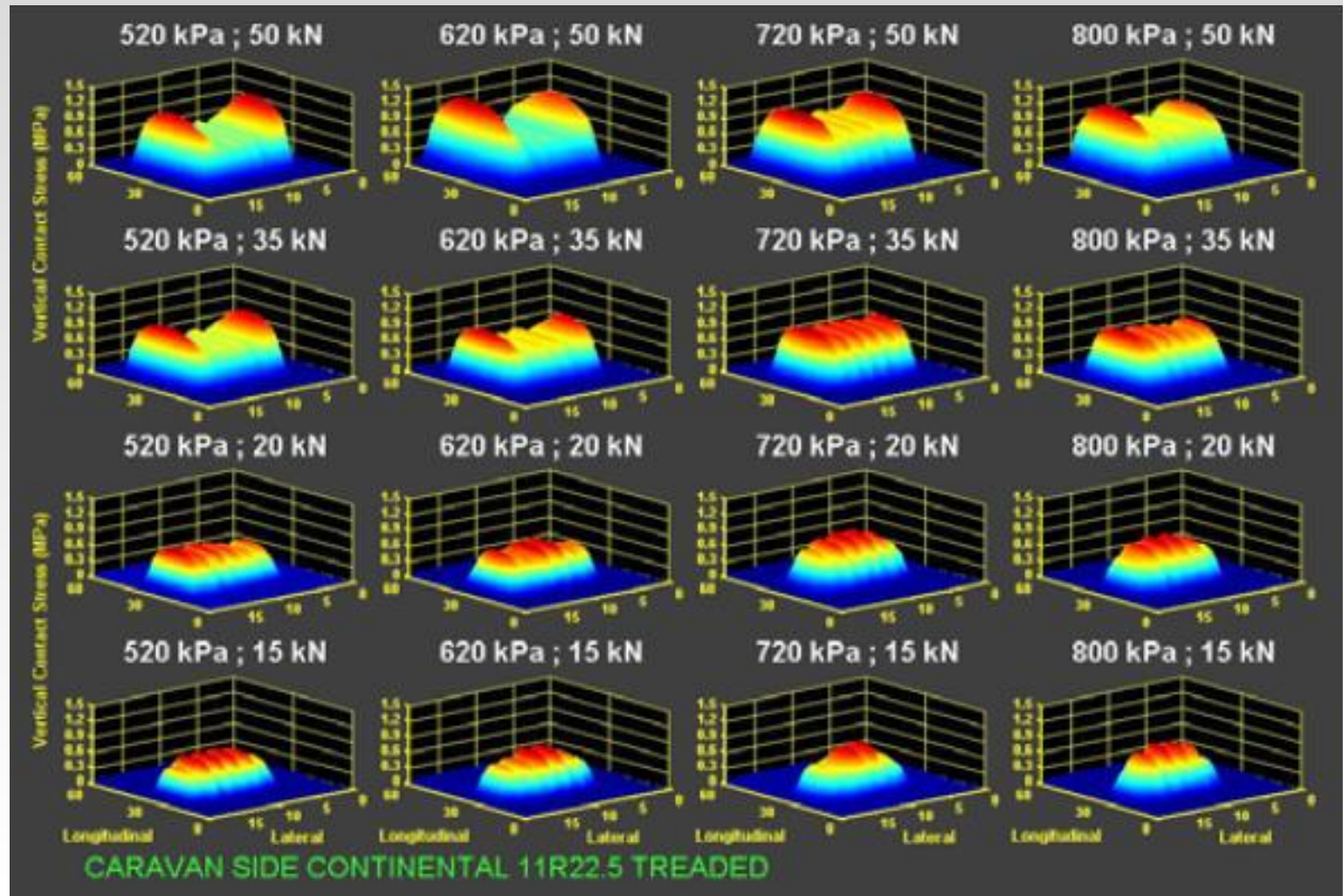
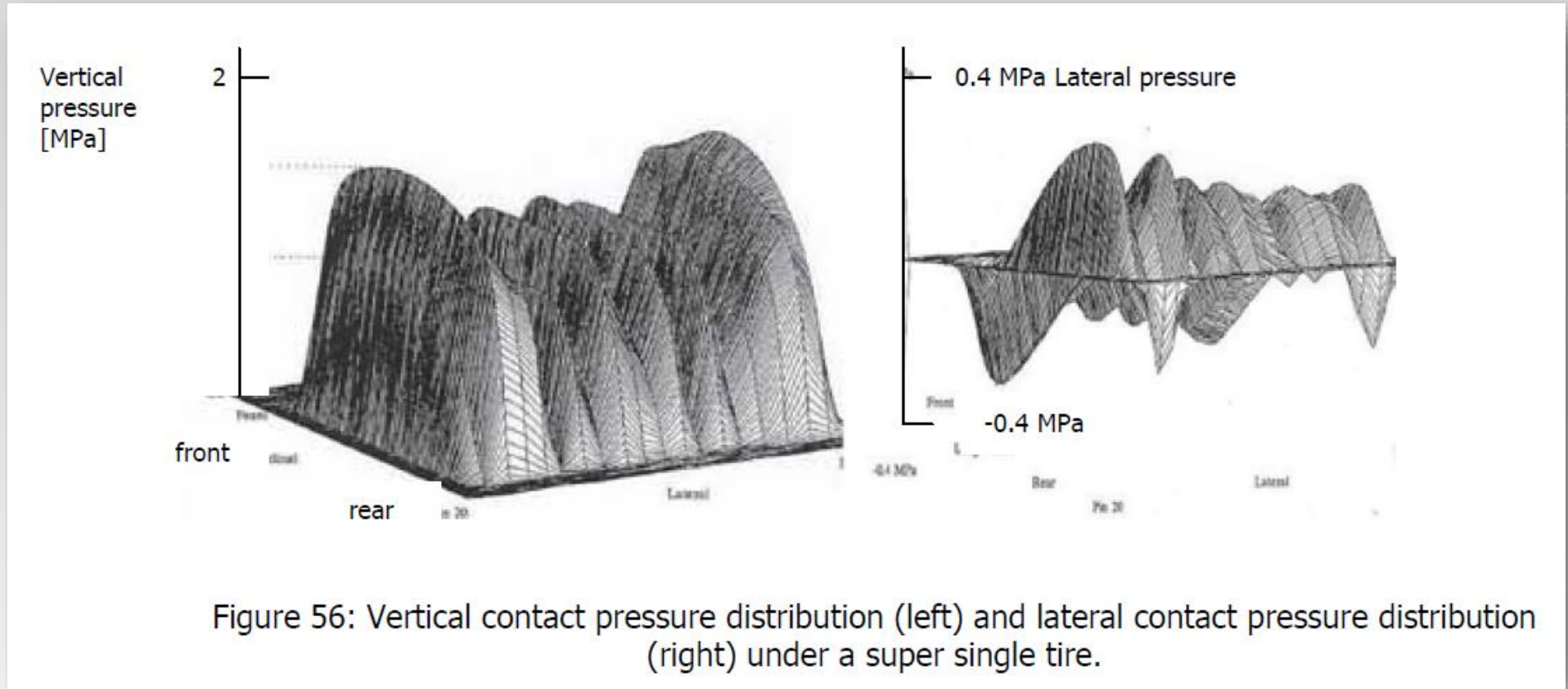


Figure 55: Vertical contact pressure distributions in relation to tire load and tire pressure.

On the other hand, if the tire load is low and the tire pressure high, the contact pressure distribution becomes more or less parabolic with the peak value at the centre of the tire.

- From the results shown in figure 55 it is obvious that too high or too low tire pressures relative to the tire load will result in excessive damage to the tire but also to the pavement surface.
- The reader should pay attention to a small detail of figure 55. One can observe that the contact area is not a circle but a rectangle.
- Furthermore one will observe that when the load increases, the length of the rectangle (driving direction) increases but the width of the rectangle remains the same.

Figure 56 shows in much more detail of the contact pressure distributions under a super single tire.



- One clearly recognizes the location of the ribs of the tire.
- Next to that one recognizes the lateral shear forces that develop under the tire as a result of the fact that the tire ribs cannot expand freely due to the friction generated by the pavement surface. It will be quite clear that these complex stress distributions should be taken into account when surface defects like raveling and rutting in the top layer need to be modeled.

- For the analysis of stresses and strains at a greater depth (more than 50 mm), modeling of the contact stresses can significantly be simplified. In such cases it is sufficient to assume a circular contact area with a homogeneously distributed contact pressure. It is common practice to assume that the contact pressure is equal to the tire pressure.
- One should realize however that this is a gross oversimplification of reality and leads to an underestimation of the stresses and strains in the top part of the pavement. This assumption should therefore only be applied if no other information is available.

If one assumes that the contact pressure is equal to the tire pressure, then the radius of the circular contact area is calculated from:

$$\pi r^2 p = F$$

Where:

r = radius of the contact area,

p = contact pressure = tire pressure,

F = wheel load.

There is however also a different method to calculate the radius of the contact area. This method is used in the design of concrete pavements. Knowing that the contact area is a rectangle in reality, an equivalent radius is calculated using:

$$a = b \sqrt{0.0028 * F + 51}$$

Where:

b = parameter dependent on the type of tire (table 11)

F = average wheel load (N) of the axle load group

Type of tire	Width of rectangular contact area(s) (mm)	Value of parameter b of equation 1	Frequency distribution (%)	
			roads	public transport bus lanes
Single tire	200	9.2	39	50
Dual tire	200	12.4	38	50
Super single tire	300	8.7	23	0
Super super single tire	400	9.1	0	0

Table 11: Value of parameter b for different tire types.

- It should be noted that the contact pressure calculated from the wheel load and the equivalent radius of the loading area is higher than the tire pressure.

A number of attempts have been made to model the contact pressure distributions under a tire. De Beer e.a. [21] have done a significant amount of work, but also the work done by Groenendijk [22] and Fernando e.a. [23] should be recognized. Based on a large number of measurements, Fernando e.a. [23] developed the computer program Tireview that allows the 3D contact pressure distributions to be calculated for a number of tires, depending on the tire load and tire pressure. They also calculated to what extent these distributions should really be taken into account meaning: at which depth is a simplified contact pressure distribution acceptable. Similar work has been done by Groenendijk [22], Myers [24] and Blab [25] and also the work done by Wardle and Gerrard [16] on this topic as well as early work done by Verstraeten [15] should be mentioned.

The results of these studies will be summarized briefly hereafter and guidance for preparing input for multi layer analyses will be given.

Based on a large number of measurements, Fernando e.a. [23] concluded that for different radial tires used in dual wheel configurations, the contact area could be calculated as follows.

Tire type	Equation to predict contact area A
215/75R17.5	$A = 36.9172 + 0.0059 T_L - 0.1965 T_p$
11R24.5	$A = 41.9417 + 0.0087 T_L - 0.2228 T_p$
11R22.5	$A = 54.4740 + 0.0066 T_L - 0.4258 T_p$
295/75R22.5	$A = 173.2141 + 0.0061 T_L - 3.1981 T_p + 0.0164 T_p^2$
A	Predicted contact area [in ²]
T _L	Tire load [lbs]
T _p	Tire inflation pressure [psi]

Table 12: Contact area for different tire types.

Fernando proposes to calculate an equivalent contact pressure, p_e , by dividing the wheel load by the predicted contact area.

$$p_e = TL / A$$

The effective radius of the contact area, r_e , is calculated following:

$$r_e = \sqrt{A / \pi}$$

- Fernando showed that this way of calculating the contact pressure and contact area had a significant effect on the magnitude of the stresses calculated in the top 50 mm of the pavement when compared with the stresses and strains calculated using the traditional approach where the contact pressure is assumed to be equal to the tire pressure. At a greater depth the differences between the two approaches became insignificant.
- Groenendijk [22] analyzed in his study the contact pressure distributions under super single tires. Just like Fernando he used the South African VRSPTA device (figure 57) to perform the contact pressure measurements. Figures 58, 59 and 60 show some typical results.

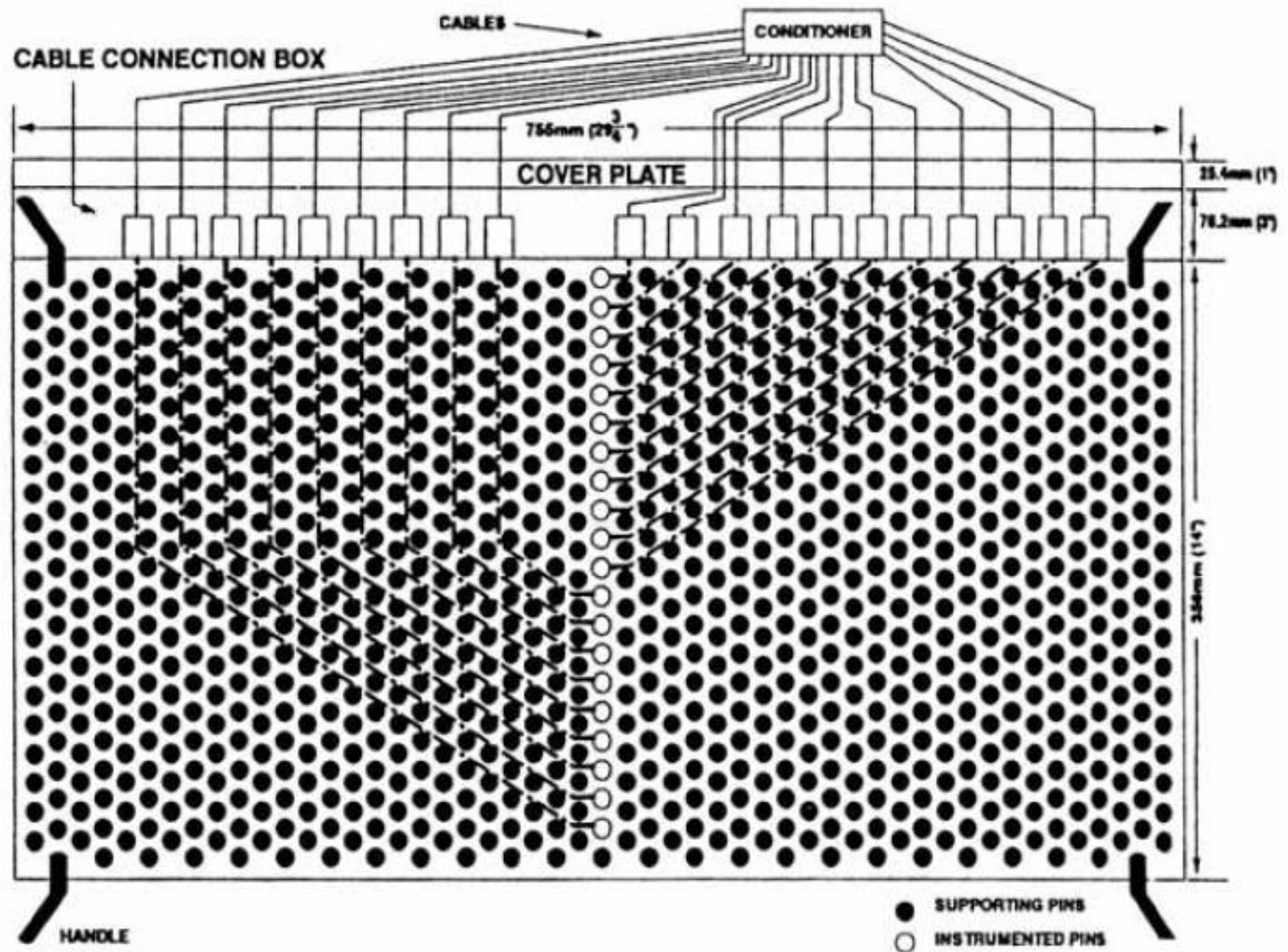


Figure 57: South African VRSPTA used for contact pressure measurements.

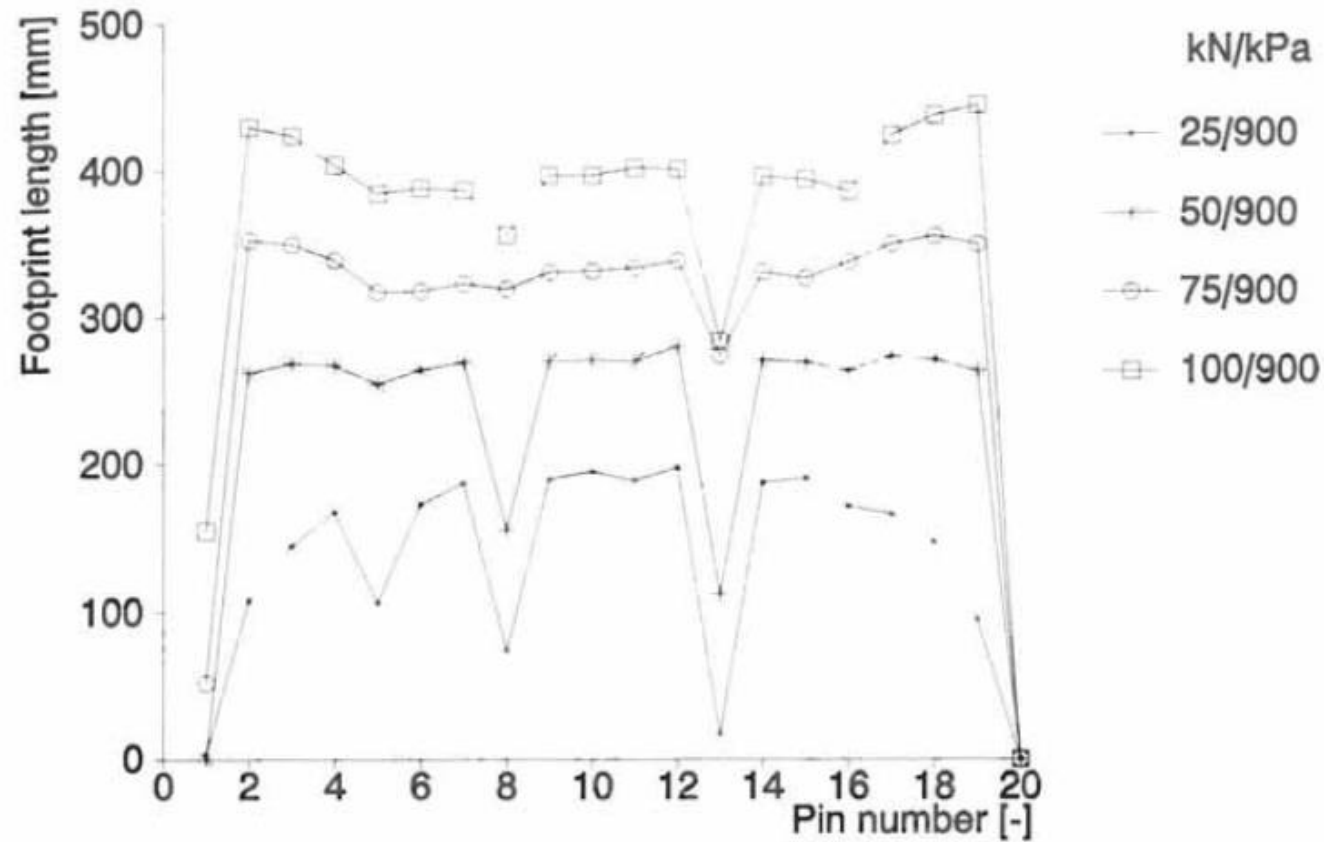


Figure 58: Foot print length of a new super single tire (R164BZ) in relation to the applied wheel load.

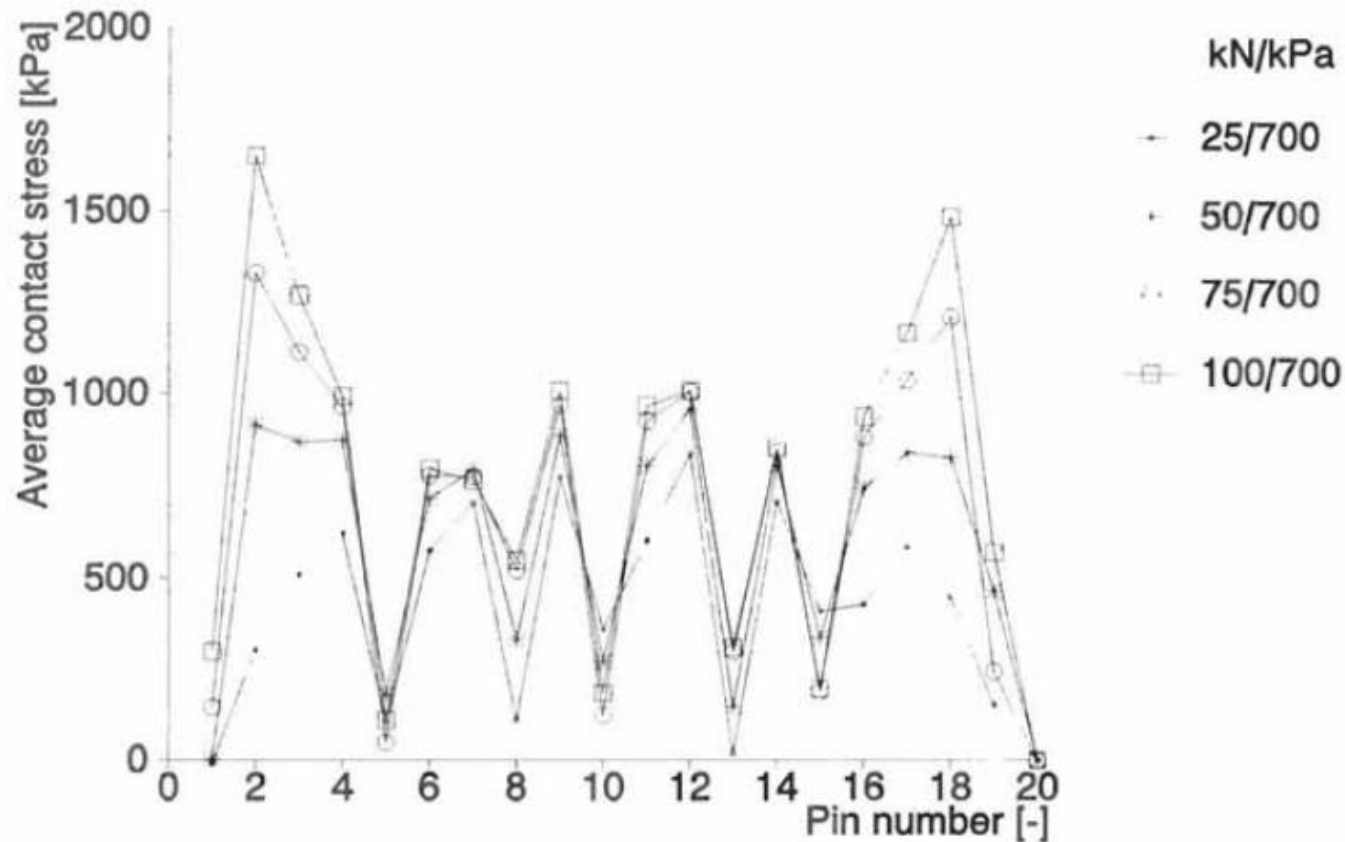


Figure 59: Variation of the vertical stresses along the width of the tire (new R164BZ) in relation to the applied wheel load.

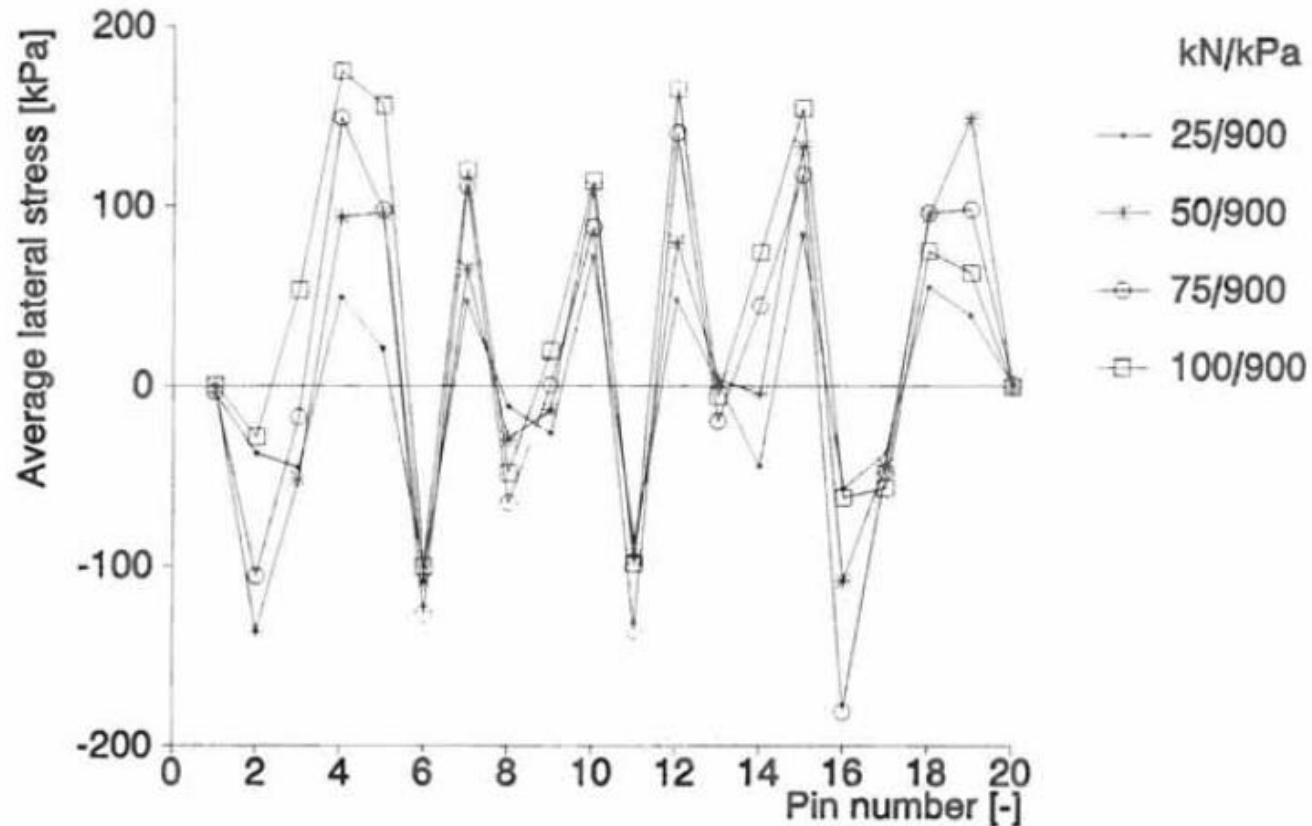


Figure 60: Variation of the transverse shear stresses along the width of the tire (new R164BZ) in relation to the applied wheel load.

Figures 61 and 62 show the longitudinal and transversal shear stress distributions as modeled by Groenendijk using the results of the contact pressure measurements.

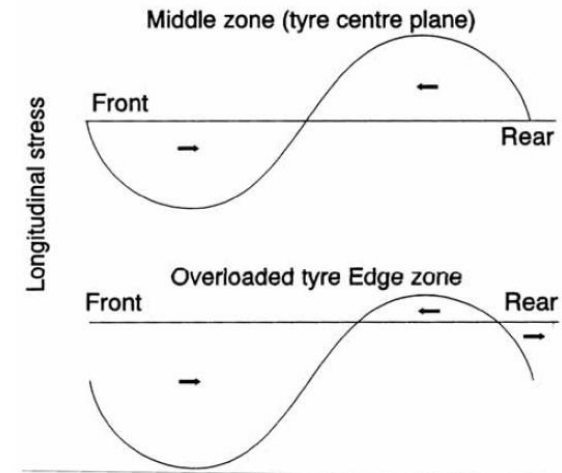


Figure 61: Modeled distribution of the longitudinal shear stresses.

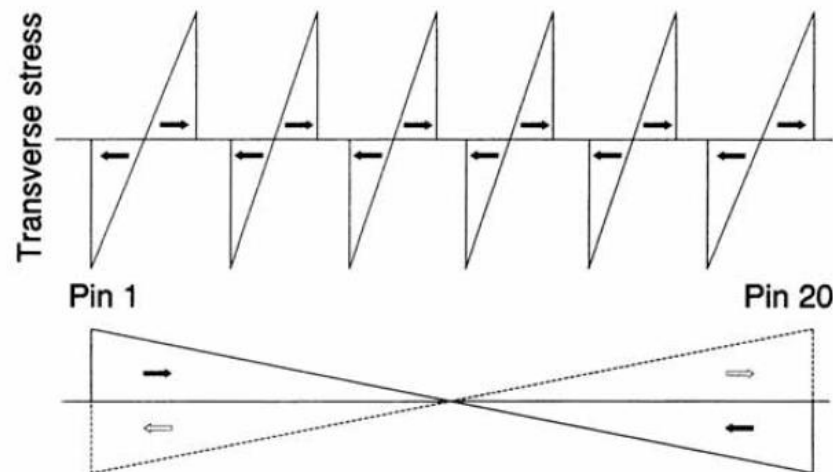


Figure 62: Modeled distribution of the transverse shear stresses. Top due to compression of the tread ribs. Bottom: due to overloading/underinflation (solid) or underloading/overinflation (dotted).

- From these figures we observe that the width of the foot print is almost independent of the wheel load, only the length of the foot print changes with changing loading conditions.
- Furthermore similar trends are observed with respect to the vertical contact pressure as shown in figures 55 and 56, being high stresses at the edge of the tire if the tire pressure is too low with respect to the wheel load and high stress in the centre of the tire when the tire is over-inflated.
- Furthermore a zigzag pattern is observed for the lateral shear stresses.

From his data, Groenendijk proposed the following equations to predict the length of the contact area and the vertical stresses and longitudinal and transversal shear stresses.

$$\begin{aligned} Z_{len} &= 115 + 5.70 F - 3.11 * 10^{-3} F p \\ Z_{aveMi} &= 422 - 1.2 F + 4.60 * 10^{-3} F p + 0.322 p + 8.60 v \\ Z_{aveEd} &= 85.5 + 9.25 F + 0.290 p + 12.9 v \\ X_{maxMi} &= 10.3 + 2.56 F - 1.15 * 10^{-3} F p + 2.50 v \\ X_{maxEd} &= 29.6 + 2.12 F - 1.19 * 10^{-3} F p + 1.96 v \\ X_{minMi} &= -30.4 - 1.55 F - 8.68 * 10^{-4} F p - 2.02 v \\ X_{minEd} &= 18.0 - 3.61 F + 1.12 * 10^{-3} F p + 0.0394 p - 3.21 v \\ Y_{ampl} &= (114 - 0.682 F + 2.05 * 10^{-3} F p) / 2 \end{aligned}$$

Where: Z_{len} = tire foot print length [mm],
 Z_{aveMi} = average vertical contact stress over the middle 60% of the tire width [kPa],
 Z_{aveEd} = average vertical contact stress over the edge 2 * 20% of the tire width [kPa],
 X_{maxMi} = maximum longitudinal shear stress averaged over the middle zone,
 X_{maxEd} = id averaged over the edge zone,
 X_{minMi} = minimum longitudinal shear stress averaged over the middle zone,
 X_{minEd} = id averaged over the edge zone
 Y_{ampl} = amplitude of the lateral shear stress zigzag pattern over the tire width [kPa],
 F = wheel load [kN],
 p = tire pressure [kPa],
 v = speed [m/s] (effect only studied for speeds up to 4 m/s !!!)

It should be noted that the contact stresses calculated using the equations given above are those acting under the tire ribs. They should not be smeared out over the entire tire footprint including the grooves! The 2 edges having a width of 20% of the entire width and don't have grooves. In the middle part there are 5 grooves c/q 4 ribs.

It will be clear that such a complex contact pressure distribution can only be properly taken into account by means of a finite element program. Also a multi layer program can be used but in that case a large number of circular loads must be used to simulate the real load. All in all it is quite clear that an as accurate as possible modeling of the load conditions is needed in order to be able to make realistic assessments of surface damage types like raveling, surface cracking and rutting in the wearing course. Therefore some suggestions to model the load are given in table 13.

Outer strip 60 mm wide	Centre strip 180 mm wide	Outer strip 60 mm wide
Length 344 mm	Length 344 mm	Length 344 mm
Area 20640 mm ² Total load 21.175 kN	Area including grooves 61920 mm ² , total load 32.65 kN Area excluding grooves approximately 48000 mm ² Meaning approximately 12000 mm ² per rib	Area 20640 mm ² Total load 21.175 kN
Model outer strip by 6 circles	Model each rib by 6 circles	Model outer strip by 6 circles
Radius 33 mm	Radius 22 mm	Radius 33 mm
Vertical uniformly distributed pressure 1026 kPa	Vertical uniformly distributed pressure 898 kPa	Vertical uniformly distributed pressure 1026 kPa

Table 13: Suggestion to model the vertical contact pressure distribution under a super single tire (F = 75 kN, p = 850 kPa).

Note: suggestions for the longitudinal and transversal shear stress distributions are not made because of the relatively low values of these stresses.

This table is based on the following assumptions. Assume a super single load of 750 kN with a tire pressure of 850 kPa. Using Groenendijk's equations we obtain the following values for the size of the loaded area, the vertical pressure and lateral shear stresses.

$Z_{len} = 344 \text{ mm}$

$Z_{aveMi} = 898 \text{ kPa}$

$Z_{aveEd} = 1026 \text{ kPa}$

$Y_{ampl} = 193 \text{ kPa}$

A close observation of the load model presented in table 13 shows that it is not that easy to comply by means of a combination of circular loads to the contact area as well as the contact pressure requirements. Better representations of the actual load conditions are possible if more circles are used.

For thickness design purposes the following approach is recommended. Determine the contact area for the tire considered using the equations provided by Fernando for tires used in dual wheel configurations and the equation provided by Groenendijk for super single tires. Calculate the effective contact pressure and the effective radius of the loading area following the procedure suggested by Fernando. For analyses of surface damage like raveling, rutting and surface cracking an as detailed as possible modeling of the actual loading conditions should be used. The data provided by Groenendijk and Myers give useful guidance in doing so.